21 ATTOSECOND OPTICS

Zenghu Chang
Department of Physics
Kansas State University
Cardwell Hall
Manhattan, Kansas

21.1 GLOSSARY

A	electric field envelope of a laser pulse
E	kinetic energy of an electron in a laser field
ε_L	electric field strength of a laser pulse at a given time
$E_{\max}$	maximum kinetic energy of an electron
ε_x	electric field strength of an attosecond XUV pulse at a given time
f_0	carrier-envelope offset frequency of a frequency comb
f_{rep}	repetition frequency of a pulse train
G	temporal gate function
φ_{CE}	carrier-envelope phase (also called absolute phase) of a laser pulse
h	Planck constant
$\hbar$	Planck constant divided by 2π
I	laser
I_p	ionization potential of an atom
λ_0	center wavelength of a laser pulse
S	trace of the frequency-resolved optical gating
τ	time delay between a laser pulse and an attosecond XUV pulse
U_p	ponderomotive potential of an electron in a laser field
ν_c	frequency of the cutoff harmonic order
ω_0	carrier angular frequency of a laser pulse

21.2 INTRODUCTION

Since the invention of the laser in 1960, the duration of coherent optical pulses has decreased from hundreds of microseconds[1,2] to 6 femtoseconds in the first 27 years.[3] Such tremendous progress was driven by the desire to generate high peak power, study dynamics in matter, increase the speed of telecommunications, and many other applications. However, by the year 1987, the optical pulse length was approaching the limit, i.e., one optical cycle of visible light, which is a few femtoseconds. The bandwidth required to support such few-cycle pulses is generated by perturbative nonlinear interactions such as self-phase modulation.

The characteristic time scale of electron motion in atoms is one atomic unit of time, which is 24.2 attoseconds. One attosecond is 10^{-18} seconds. In the Bohr's model of the atom, the electron orbital time around the hydrogen nucleus is 152 attoseconds. The study of electron dynamics in atoms and molecules called for optical pulses with attosecond duration.[4–6] In the frequency domain, a transform-limited Gaussian pulse with 24 attosecond full width at half maximum (FWHM) corresponds to a 73 eV FWHM power spectrum, which is much broader than the entire visible light range. In other words, attosecond pulses are inherently XUV light or x rays. The duration of such extremely short pulses was first measured in 2001.[7,8] The required ultrabroad spectrum was obtained by using a nonperturbative nonlinear optics process called high-order harmonic generation, discovered in 1987–1988.[9,10]

High Harmonic Generation

When a linearly polarized, short-pulse laser beam with an intensity on the order of 10^{14} W/cm^2 interacts with noble gases, odd harmonics of the fundamental frequency—up to tens or even hundreds in order—emerge in the output beam,[11,12] as depicted in Fig. 1. The intensity of the first few order harmonics decreases quickly as the order increases, then the intensity remains almost unchanged over many harmonic orders, forming a plateau. Finally, the signal cuts off abruptly at the highest order. The broad width of the plateau provided the required spectral bandwidth to support attosecond pulses. The appearance of the intensity plateau is the signature of this nonperturbative laser-atom interaction, which can be described by a semiclassical model.

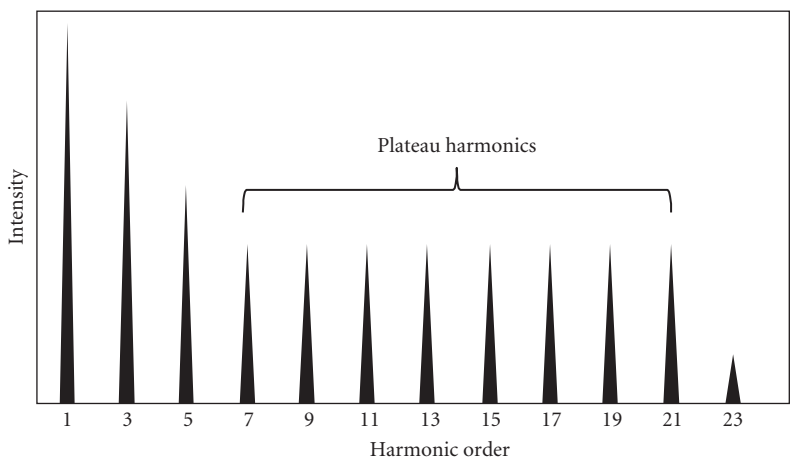

FIGURE 1 High-order harmonic spectrum.

Semiclassical Model

It is also called three-step or two-step model, rescattering model. The electric field acting on an atom changes sinusoidally within one laser cycle. As the laser intensity reaches the level of 10^{14} W/cm^2, the field near the peak of the oscillation is comparable to the atomic Coulomb field. The superposition of the laser field and the Coulomb field transforms the potential well that binds the electron into a potential barrier. As a result, the electron in the ground state tunnels through the barrier (the first step). The freed electron moves in the laser field like a classical particle and its trajectory can be calculated using Newton's second law. In one laser cycle, the electron first moves away from the nucleus, then is driven back when the force changes direction. During the returning journey, the electron can acquire kinetic energy up to hundreds of electron volts (the second step). Finally, the electron recombines with the parent ion with the emission of a photon (the third step).[13,14]

When all electrons released near one peak of a laser cycle are considered, the emitted photons form an attosecond pulse. Since there are two field maxima in one laser cycle, two attosecond pulses are generated. For a laser pulse that contains many cycles, an attosecond pulse train is produced. The pulse train corresponds to discrete harmonic peaks in the frequency domain. In other words, high harmonic generation and the attosecond pulse train are two manifestations of the same nonperturbative interaction.

The photon energy of the cutoff harmonic order, $h\nu_c$, is determined by the maximum kinetic energy of the electron gained in the laser field, $E_{\max}$. It can be shown that $h\nu_c = I_p + E_{\max} \approx I_p + 3U_p$. Here I_p is the ionization potential of the atom and U_p is the ponderomotive potential of the electron in the laser field. Apparently, the width of the plateau and therefore the minimum attosecond pulse duration is limited by $h\nu_c$. The cutoff order is also affected by the depletion of the ground state population due to the ionization.[15]

Ponderomotive Potential

The ponderomotive potential is the cycle-averaged kinetic energy of an electron in a laser field, $U_p[eV] = 9.33 \times 10^{-14} I \cdot \lambda_0^2$, where I is the laser intensity in W/cm^2 and λ_0 is the center wavelength of the laser in micrometer. It is clear that the cutoff photon energy of the high harmonic spectrum can be extended by using longer wavelength driving lasers.[16]

Strong Field Approximation

A fully quantum three-step model was developed in 1994.[17] It is valid when the ponderomotive potential is much larger than the ionization potential. It assumes that the harmonic emission is the result of the dipole transition between the ground state and the continuum states only, with the excitation states playing no role. Solving the Schrödinger equation results in an analytical solution of the dipole moment, from which one can obtain both the phase and the intensity of each harmonic order. The model reveals that there are two quantum trajectories that contribute to each plateau harmonic. One is called the long trajectory and the other is the short trajectory. The phase of each harmonic depends on the laser intensity. The intensity dependence of the dipole phase (also called intrinsic phase) is different for the two trajectories.

Quantum Trajectories

By solving the equation of motion, it can be shown that an electron released right at the peak of the laser field will return to the starting point one cycle later, with zero kinetic energy. As the releasing time from the field peak increases, the returning energy increases first, reaches the maximum value ($3\ U_p$), then decreases to zero. Therefore electrons releasing at two different moments can come back to the parent ion with the same kinetic energy, which corresponds to the same harmonic order.[13,14]

The electron that starts the journey earlier returns later. Its path is called the long trajectory. The other one is the short trajectory. Quantum mechanically, there are many trajectories contribute to each harmonics (Feynman's path-integral), but the dominating contributions are from the two trajectories corresponding to the classical ones.[17]

Phase-Matching

The semiclassical model and the strong field approximation describe the single atom response. To generate a high-intensity high harmonic beam, many atoms must contribute to the output constructively.[18] Ionization of the atom is unavoidable in high harmonic generation because it is the first step of the process. In highly ionized gas targets, the phase velocity of the laser field (and thus the polarization) is greater than that of the harmonic field. The resulting phase mismatch can be compensated for by several approaches. One of them utilizes the intensity dependent phase.[19] In most cases, only the short trajectory is phase matched. Nevertheless, low laser to harmonic conversion efficiency is still a major problem that needs to be solved. The spatial coherence of the high harmonic/attosecond train beam is excellent when the phase matching conditions are fulfilled. The divergence angle of the XUV beam is smaller than the driving laser beam.[12]

Single Isolated Pulses

The attosecond pulse train corresponding to high order harmonics is useful for some applications. In general, however, single isolated attosecond pulses are required for performing pump-probe experiments with arbitrary delay between the pump and the probe pulses. Such pulses can be generated by suppressing all the pulses in the train except one, which can be accomplished by using single-cycle driving lasers[20] or pulse extraction switches with a subcycle opening time.[21] Also the pulses from the gas target are positively chirped.[22] Dispersion compensation over a broad XUV spectral range is a major challenge. By 2008, the shortest single isolated pulses, which were generated from neon gas by using 3.3-fs driving lasers centered at 720 nm, were 80 attoseconds and contained ~0.5 nJ of energy.[23] Their spectrum was centered at 80 eV.

21.3 THE DRIVING LASER

There are several basic requirements on the driving lasers for the generation of single isolated attosecond pulses. First, the intensity at the focus must be high enough, on the order of 10^{14} to 10^{15} W/cm^2, which is a faction of an atomic unit of intensity (3.55×10^{16} W/cm^2). The corresponding pulse energy is 100 μJ or higher. The spectral bandwidth of the attosecond pulses is proportional to the driving laser intensity. Second, the laser pulse duration must be short enough. The ionization of the target atoms by the laser field before the cycle where the attosecond pulse is generated must not deplete the ground state population completely. Depending on the generation scheme, acceptable laser pulses range from 3 to 30 fs. Third, the carrier-envelope phase needs to be stabilized. Since the single attosecond pulses are generated in a faction of the laser cycle, a shift in the carrier-envelope phase results in shot-to-shot variations of the attosecond pulses. Finally, the repetition rate of the laser should be high, on the order of kilohertz. Many attosecond characterization and application schemes rely on photoelectron measurements. There is an upper limit on the number of electrons per shot to avoid the space charge effect. Thus the signal count rate is primarily determined by the repetition rate. The energy stability of high-repetition-rate lasers is also better than those with low repetition rates.

High power lasers pulses with duration around 30 fs can be generated with chirped pulse amplification. Pulses down to ~4 fs with submillijoule energy can be obtained by spectral broadening in hollow-core fibers filled with gases, followed by dispersion compensation using chirped mirrors or phase modulators,[24–27] as illustrated by the block diagram in Fig. 2.

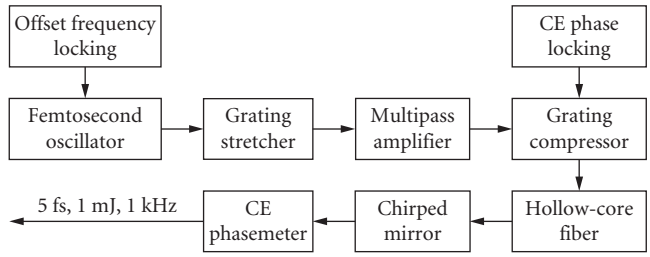

FIGURE 2 A carrier-envelop phase stabilized, few-cycle laser system.

Chirped Pulse Amplification (CPA)

Ti:Sapphire is a commonly used gain medium for femtosecond lasers primarily because of its broad gain bandwidth.[28] Its center wavelength is ~800 nm, which corresponds to a ~2.6-fs optical period. Femtosecond oscillators that use Ti:Sapphire as the gain medium can generate pulses with nanojoule level energy. Direct amplification of the pulse to millijoule level may cause damage to the laser crystal. In a chirped amplifier, the pulses from the oscillator are stretched to hundreds of picoseconds to lower the peak power. Then the pulses are amplified in multipass or regenerative amplifiers. The high energy pulses are finally compressed to femtosecond duration.[29,30] Most high energy (>5 mJ) lasers use grating pairs to stretch and compress pulses.

Carrier-Envelope Phase

The effects of the magnetic field of the laser on high harmonic generation can be ignored because the electron velocity during the three-step journey is much slower than the speed of light. The electric field of a linearly polarized laser pulse can be expressed as $\varepsilon_L(t) = A(t)\cos(\omega_0 t + \varphi_{CE})$. Here $A(t)$ is the pulse envelope, ω_0 is the carrier frequency, φ_{CE} is the carrier-envelope (CE) phase that specifies the offset between the peak of the pulse envelope and the closest maximum of the oscillating field. To stabilize the carrier-envelope phase of the laser pulses from chirped pulse amplifiers followed by the hollow-core fiber compressors, the carrier-envelope offset frequency of the oscillator must first be stabilized. Furthermore, the CE phase drifts in the chirped pulse amplifier and in the hollow-core fiber compressor must be compensated.[31,32]

Carrier-Envelope Offset Frequency

The technique for stabilizing carrier-envelope offset frequency was originally developed for frequency metrology in 2000.[33,34] Most femtosecond oscillators used for seeding amplifiers work at a repetition rate f_{rep} ~80 MHz. The oscillator output is a femosecond pulse train that corresponds to a frequency comb. The frequency of the nth tooth of the comb is $f_0 + nf_{rep}$, where f_0 is the frequency of the zeroth tooth. The rate of carrier-envelope phase change is determined by the offset frequency f_0, which can be stabilized by using f-to-$2f$ technology. For this to work, the laser spectrum must cover an octave. The f_0 is measured by beating the $2n$th tooth with the frequency doubled nth tooth, that is $f_0 = 2[f_0 + nf_{rep}] - (f_0 + 2nf_{rep})$. It was found that f_0 can be stabilized by controlling the pump power to the gain medium of chirped mirror based oscillators. When f_0 is fixed to f_{rep}/m, the CE phase of every mth pulse from the oscillator is the same. It is common practice to choose $m = 4$.

Carrier-Envelope Phase of Chirped Pulse Amplifiers

The oscillator pulses with the same CE phase are switched out by a Pockels cell and sent to Ti:Sapphire amplifiers that operate at kilohertz repetition rates. When grating pairs are used to stretch and compress laser pulses for the chirped pulse amplification, a submicrometer change of separation between gratings can lead to a 2π CE phase shift.[35] This effect has been used to correct the slow CE phase variation introduced by the amplifier components. It was accomplished by measuring the CE phase variation after the amplifier and using the measured signal for feedback control of the grating separation.[36] The CE phase error of CPA systems can be controlled to <200 mrad over hours. The relative CE phase variation can be measured by a single shot *f*-to-2*f* interferometer, whereas the absolute phase value can be determined by a phasemeter (discussed below), which measures electrons from the above-threshold ionization of atoms by the laser pulses.

Single Shot *f*-to-2*f* Interferometer

The laser pulse from the hollow-core fiber compressor is a white-light continuum that can cover an octave spectral range. One can select a narrow range near 1000 nm and frequency double it to interfere with the light around 500 nm. The interferogram in the frequency domain is a sinusoidal fringe. The period of the fringe pattern is inversely proportional to the delay between the two interfering pulses. A CE phase shift will cause the fringes to shift. Thus by measuring the interferogram with a spectrometer, the CE phase variation can be measured.[37]

Carrier-Envelope Phasemeter

In the three-step semiclassical model, the attosecond photon pulses are generated by the recombination of the returning electrons. A returning electron can also scatter away from the parent ion. The kinetic energy distribution of the rescattered electrons after the laser field vanishes can extend to $10U_p$. There is also a plateau in the electron spectrum similar to the high harmonic spectrum. This electron emission process is called above-threshold ionization. The angular distribution of the electrons is concentrated along the field polarization direction. When the laser pulse is only a few cycles long, the number of plateau electrons flying to one direction can be different from those to the opposite direction. The asymmetry depends on the carrier-envelope phase of the laser. Thus, by simultaneously measuring electrons in two directions, the absolute CE phase value can be determined.[38]

21.4 ATTOSECOND PULSE GENERATION

A typical attosecond pulse generation setup consists of a kilohertz femtosecond Ti:Sapphire laser system, a vacuum chamber where the gas target is located, and an XUV spectrometer/attosecond streak camera that characterizes the pulses in the spectral domain and the time domain, as shown in Fig. 3. The attosecond pulses are XUV or soft x-ray light that cannot propagate in air because of high absorption. The gas density in the laser interaction region is on the order of 10^{17} to 10^{18} atoms/cm^3. The interaction length is typically a few millimeters for gas cells or gas jets. It should be smaller than the Rayleigh range of the focusing laser beam, so that the carrier-envelope phase does not change significantly due to the Gouy phase shift inside the target. The target is located after the focal point to achieve good phase-matching.

Attosecond Pulse Train

Such pulses are generated with linearly polarized laser pulses that contain many optical cycles. When only the fundamental frequency is used, the spacing between two neighboring harmonic

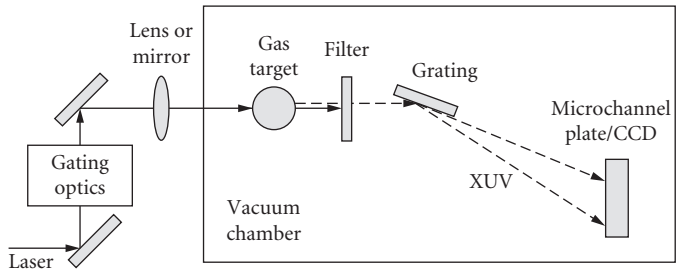

FIGURE 3 Setup for generating attosecond pulses and measuring their spectrum.

peaks is two-photon energies. In the time domain, the spacing between adjacent pulses is one-half of an optical cycle; 1.3 fs for Ti:Sapphire lasers.[7,39] The amplitude changes from pulse to pulse. Since many-cycle lasers (>20 fs) can be generated directly from high power (terawatt) chirped pulses amplifiers, the attosecond pulse energy can be high enough to perform nonlinear physics experiments.[40]

Two-Color Gating

When the many-cycle driving laser is a combination of the fundamental frequency and its second harmonic, the breaking of symmetry of the laser field leads to the generation of both odd and even high harmonics and thus the spacing between two neighboring harmonic peaks is one photon-energy. In the time domain, the spacing between adjacent pulses becomes a full optical cycle.[41] Such pulse trains are useful for performing experiments using the powerful attosecond streaking technique.

Amplitude Gating

As the driving laser approaches a single optical cycle, the cycle-to-cycle field amplitude variation becomes significant. When the carrier-envelope phase of the pump laser is set to zero, the spectrum of the attosecond pulses generated near the peak of the laser pulse envelope extends to a shorter XUV wavelength range as compared to the adjacent attosecond pulses emitted when the laser field is weaker. As a result, the high-order harmonic spectrum becomes a continuum in the cutoff region.[20] Discrete harmonics remain in other portions of the spectrum. The shorter the driving laser is, the broader the XUV continuum becomes. A single isolated attosecond pulse as short as 80 attoseconds was obtained by selecting the continuum region of the XUV spectrum with a high-pass filter, using <4-fs pump lasers.[21] The scaling of the attosecond pulse energy is limited by the maximum energy of the driving laser from the hollow-core fiber compressor. Combining this type of gating with the two-color gating can relax the requirement of the laser pulse duration.

Polarization Gating

In the plateau region, four attosecond pulses are produced in one laser cycle taking into account both the long and short trajectory's contributions. However, only the two pulses from the short trajectory can be phase matched on axis. Consequently, the spacing between pulses is still half of a laser cycle. Single isolated attosecond pulses can be extracted by a scheme called polarization gating.[21] It uses a laser field with a rapid change of ellipticity. Since XUV attosecond pulses can only be efficiently generated with linearly polarized driving fields, a single attosecond pulse is emitted if the laser field

is linearly polarized in only a short time range and elliptically polarized in the other portion of the driving pulse. The time range over which the attosecond pulse is generated is called the polarization gate. So far, single isolated XUV pulses as short as 130 attoseconds were generated with this method using 5 fs pump lasers.[42] For the same driving laser pulse duration, polarization gating has the potential to generate shorter attosecond pulses because it can create a broader continuum in the plateau region.[43]

Double Optical Gating

The few-cycle laser pulses used in amplitude gating and polarization gating are difficult to generate daily. A method called double optical gating was proposed to allow the generation of single isolated attosecond pulses with longer pump lasers.[44] It is a combination of the two-color gating and the polarization gating. A second harmonic field is added to the fundamental field in order to break the symmetry of the field and increases the spacing between the adjacent attosecond pulses to one optical cycle. When the polarization gating is applied, the polarization gate width equals one optical cycle to select one isolated XUV pulse. The depletion of the ground state population by the leading edge of the laser pulses can be significantly reduced with this scheme; as a result, multicycle lasers can be used. This scheme has been demonstrated with laser pulses as long as 20 fs. Since such lasers do not necessarily need hollow-core fiber compressors, they are much easier to operate. The laser pulse energy can also be much higher, which is important for the energy scaling of the attosecond pulses.

21.5 ATTOSECOND PULSE CHARACTERIZATION

Measurement of the optical pulse duration requires a temporal gate. For femtosecond lasers, nonlinear optics phenomena such as second harmonic generation can serve as the gating, which is the foundation of widely implemented autocorrelation and the frequency-resolved optical gating (FROG) techniques.[45] The intensity of the attosecond pulses is not high enough to generate second harmonic light yet. Most of the methods for determining the width of the attosecond pulses require the measurements of photoelectrons or ions. The XUV beam is focused to a gas target to generate the photoelectrons/ions. The charged particles are detected by a time-of-flight spectrometer. A second beam, either an XUV or an intense laser beam is also focused to the same target, overlapping spatially and temporally with the first beam. The interaction of the two pulses in the gas serves as the temporal gate. A typical setup is shown in Fig. 4, where the attosecond XUV pulses are generated in the first gas target and are measured in the second gas target. Similar apparatus have been used for studying electron dynamics in atoms.

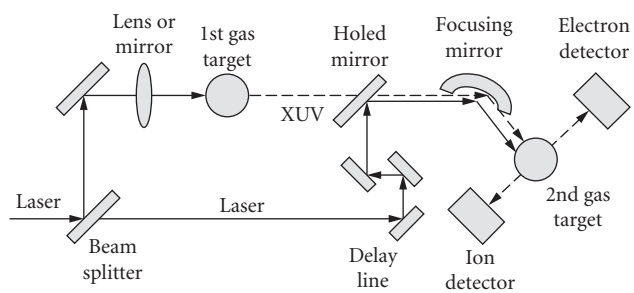

FIGURE 4 Setup for measuring the attosecond pulse duration.

Second-Order Autocorrelator or FROG

This technique resembles the second harmonic autocorrelation in femtosecond optics. Ionization of atoms (such as helium) or Coulomb explosion of molecules (such as N_2) by nonresonant two-photon absorption can serve as the nonlinearity. The ion signal as a function of the time delay between the two attosecond pulses is measured to yield the second order autocorrelation function.[40] By assuming a certain pulse shape, the pulse duration can be obtained by fitting the autocorrelation trace. The interferometric second-order autocorrelations have been used to characterize attosecond pulse trains generated with low-repetition rate femtosecond lasers with tens of millijoule pulse energy.

When the photoelectron kinetic energy spectrum is measured as a function of the delay, a two-dimensional frequency-resolved optical gating pattern is obtained. Both the phase and pulse profile of subfemtosecond pulses can be reconstructed using this method.[46]

RABITT (Reconstruction of Attosecond Beating by Interference of Two-Photon Transition)

When the attosecond pulse train is generated with the fundamental wave of kilohertz lasers, the intensity of the XUV light may not be strong enough to cause measurable nonlinear effects. A cross-correlation method based on the two-color above-threshold ionization was developed to determine the duration of the pulses in the train.[7] A high harmonic beam interacting with atomic gases alone will generate photoelectron peaks separated by two laser photon-energies. Adding a dressing laser with intensity of 10^{11} W/cm^2 generates an electron sideband located in the middle of two peaks. By measuring sideband intensity as a function of the delay between the XUV pulse and the dressing laser, relative phase between adjacent harmonics can be determined. Combining this with the high harmonic power spectrum, one can deduce the attosecond pulse duration. This approach assumes that the width of all the pulses in the train is the same.

Attosecond Streak Camera

The photoelectron replicas generated by attosecond XUV pulses have durations shorter than the optical cycle of the driving lasers. When the photoelectrons are released in the presence of a laser field, their momentum after the laser pulse is gone will be different from the initial value. The momentum shift is determined by the vector potential of the laser field at the time the electron is released. Thus, the leading edge of the electron pulse will gain an additional momentum that is different from the electron in the trailing edge. By measuring the momentum distribution of photoelectrons, the width of the photoelectron pulse (and thus the XUV pulse) can be determined.[47,48] The required laser intensity is on the order of 10^{12} to 10^{13} W/cm^2. This approach is similar to the picosecond optical streak camera. It has been used to measure single isolated attosecond pulses and the pulse trains generated from the two-color gating. It is, however, difficult to measure pulses with half laser cycle spacing with this method.

FROG-CRAB (Frequency-Resolved Optical Gating for Complete Reconstruction of Attosecond Bursts)

The momentum streaking of the photoelectrons in a laser field can also be described as the phase shift of an electron wave packet. The phase shift of the electron wave by the laser field can be considered as a temporal phase gate, $G(t)$. When the photoelectron spectrum is measured as a function of the delay τ between the XUV field $\varepsilon_x(t)$ and the laser field, a FROG trace is obtained, given by $S(E,\tau)=\left|\int_{-\infty}^{\infty} dt\varepsilon_x(t-\tau)G(t)e^{j(E+I_p)t/\hbar}\right|^2$. Here E is the energy of the photoelectron. Such a spectrogram can be processed using a FROG retrieval algorithm to fully characterize the XUV pulse as well as the electric field of the near IR laser pulse.[49,50] This method works well for measuring both attosecond pulse trains and single isolated pulses.

21.6 ACKNOWLEDGMENTS

This material is supported by the U.S. Army Research Office under grant number W911NF-07-1-0475.

21.7 REFERENCES

1. T. H. Maiman, "Stimulated Optical Radiation in Ruby," *Nature* **187:** 493–494 (1960).
2. A. E. Siegman, *Lasers*, University Science Books, Mill Valley, California (1986), ISBN 0-935702-11-3, p. 61.
3. R. L. Fork, C. H. B. Cruz, P. C. Becker, and C. V. Shank, "Compression of Optical Pulses to Six Femtoseconds by Using Cubic Phase Compensation," *Opt. Lett.* **12:** 483–485 (1987).
4. P. Agostini, and L. F. DiMauro, "The Physics of Attosecond Light Pulses," *Reports on Progress in Physics* **67:** 813 (2004).
5. P. B. Corkum and F. Krausz, "Attosecond Science," *Nat. Phys.* **3:** 381 (2007).
6. M. F. Kling and M. J. J. Vrakking, "Attosecond Electron Dynamics," *Annual Review of Physical Chemistry* **59:** 463 (2008).
7. P. M. Paul, E. S. Toma, P. Breger, G. Mullot, F. Auge, Ph. Balcou, H. G. Muller, and P. Agostini, "Observation of a Train of Attosecond Pulses from High Harmonic Generation," *Science* **292:** 1689 (2001).
8. M. Hentschel, R. Kienberger, Ch. Spielmann, G. A. Reider, N. Milosevic, T. Brabec, P. Corkum, U. Heinzmann, M. Drescher, and F. Krausz, "Attosecond Metrology," *Nature* **414:** 509 (2001).
9. A. McPherson, G. Gibson, H. Jara, U. Johann, T. S. Luk, I. A. McIntyre, K. Boyer, and C. K. Rhodes, "Studies of Multiphoton Production of Vacuum-Ultraviolet Radiation in the Rare Gases," *J. Opt. Soc. Am. B* **4:** 595 (1987).
10. M. Ferray, A. L'Huillier, X. F. Li, L. A. Lompré, G. Mainfray, and C. Manus, "Multiple-Harmonic Conversion of 1064 nm Radiation in Rare Gases," *J. Phys. B* **21:** L31 (1988).
11. A. L'Huillier, T. Auguste, Ph. Balcou, B. Carŕe , P. Monot, P. Salières, C. Altucci, et al.,"High-Order Harmonics: A Coherent Source in the XUV Range," *J. Nonl. Opt. Phys. and Mat.* **4:** 647 (1995).
12. P. Salières, A. L'Huillier, P. Antoine, M. Lewenstein, "Studies of the Spatial and Temporal Coherence of High Order Harmonics," *Adv. Atom. Mol. Opt. Phys*. **41:** 83 (1999).
13. P. B. Corkum, "Plasma Perspective on Strong-Field Multiphoton Ionization," *Phys. Rev. Lett.* **71:** 1994–1997 (1993).
14. K. C. Kulander, K. J. Schafer, J. L. Krause, in Super-Intense Laser-Atom Physics, B. Piraux, A. L'Huillier, and K. Rzazewski (eds.) Plenum, New York (1993). NATO ASI, Ser. B, Vol. **316:** p. 95.
15. Z. Chang, A. Rundquist, H. Wang, M. M. Murnane, and H. C. Kapteyn, "Generation of Coherent Soft X Rays at 2.7 nm Using High Harmonics," *Phys. Rev. Lett.* **79:** 2967 (1997).
16. B. Shan, Z. Chang, "Dramatic Extension of the High-Order Harmonic Cutoff by Using a Long-Wavelength Pump," *Phys. Rev. A* **65:** 011804(R) (2002).
17. M. Lewenstein, Ph. Balcou, M. Yu. Ivanov, A. L'Huillier, and P. B. Corkum, "Theory of High-Harmonic Generation by Low-Frequency Laser Fields," *Phys. Rev. A* **49:** 2117–2132 (1994).
18. M. B. Gaarde, J. L. Tate, and K. J. Schafer, "Macroscopic Aspects of Attosecond Pulse Generation," *J. Phys. B: At. Mol. Opt. Phys.* **41:** 32001 (2008).
19. M. Lewenstein, P. Salières, and A. L'Huillier "Phase of the Atomic Polarization in High-Order Harmonic Generation," *Phys. Rev. A* **52:** 4747 (1995).
20. I. P. Christov, M. M. Murnane, and H. Kapteyn, "High-Harmonic Generation of Attosecond Pulses in the 'Single-Cycle' Regime," *Phys. Rev. Lett.* **78:** 1251–1254 (1997).
21. P. B. Corkum, N. H. Burnett, and M. Y. Ivanov, "Subfemtosecond Pulses," *Opt. Lett.* **19:** 1870 (1994).
22. Z. Chang, "Chirp of the Attosecond Pulses Generated by a Polarization Gating," *Phys. Rev. A* **71:** 023813 (2005).
23. E. Goulielmakis, M. Schultze, M. Hofstetter, V. S. Yakovlev, J. Gagnon, M. Uiberacker, A. L. Aquila, et al., "Single-Cycle Nonlinear Optics," *Science* **320:** 1614 (2008).
24. M. Nisoli, S. D. Silvestri, and O. Svelto, "Generation of High Energy 10 fs Pulses by a New Pulse Compression Technique," *Appl. Phys. Lett.* **68:** 2793–2975 (1996).

25. R. Szipöcs, K. Ferencz, C. Spielmann, and F. Krausz, "Chirped Multilayer Coatings for Broadband Dispersion Control in Femtosecond Lasers," *Opt. Lett.* **19:** 201–203 (1994).
26. M. Nisoli, S. D. Slverstri, O. Svelto, R. Szipöcs, K. Ferencz, Ch. Spielmann, S. Sartania, and F. Krausz, "Compression of High-Energy Laser Pulse below 5 fs," *Opt. Lett.* **22:** 522–524 (1997).
27. H. Wang, Y. Wu, C. Li, H. Mashiko, S. Gilbertson, and Z. Chang, "Generation of 0.5 mJ, Few-Cycle Laser Pulses by an Adaptive Phase Modulator," *Opt. Exp.* **16:** 14448–14455 (2008).
28. P. F. Moulton, "Spectroscopic and Laser Characteristics of Ti:Al_2O_3," *J. Opt. Soc. Am. B* **3:** 125 (1986).
29. D. Strickland and G. Mourou, "Compression of Amplified Chirped Optical Pulses," *Opt. Commun.* **56:** 219 (1985).
30. G. A. Mourou, T. Tajima, and S. V. Bulanov, "Optics in the Relativistic Regime," *Rev. Mod. Phys.* **78:** 309 (2006).
31. A. Baltuska, Th. Udem, M. Uiberacker, M. Hentschel, E. Goulielmakis, Ch. Gohle, R. Holzwarth, et al., "Attosecond Control of Electronic Processes by Intense Light Fields," *Nature* **421:** 611 (2003).
32. A. Baltuška, M. Uiberacker, E. Goulielmakis, R. Kienberger, V. S. Yakovlev, T. Udem, T. W. Hänsch, and F. Krausz, "Phase-Controlled Amplification of Few-Cycle Laser Pulses," *IEEE J. Sel. Topics Quantum Electron*. **9:** 972 (2003).
33. D. J. Jones, S. A. Diddams, J. K. Ranka, A. Stentz, R. S.Windeler, J. L. Hall, and S. T. Cundiff, "Carrier-Envelope Phase Control of Femtosecond Mode-Locked Lasers and Direct Optical Frequency Synthesis," *Science* **288:** 635–639 (2000).
34. A. Apolonski, A. Poppe, G. Tempea, C. Spielmann, T. Udem, R. Holzwarth, T. W. Hänsch, and F. Krausz, "Controlling the Phase Evolution of Few-Cycle Light Pulses," *Phys. Rev. Lett.* **85:** 740–743 (2000).
35. Z. Chang, "Carrier Envelope Phase Shift Caused by Grating-Based Stretchers and Compressors," *Appl. Opt.* **45:** 8350(2006).
36. C. Li, E. Moon, and Z. Chang, "Carrier-Envelope Phase Shift Caused by Variation of Grating Separation," *Opt. Lett.* **31:** 3113–3115 (2006).
37. M. Kakehata, H. Takada, Y. Kobayashi, K. Torizuka, Y. Fujihara, T. Homma, and H. Takahashi, "Single-Shot Measurement of Carrier-Envelope Phase Changes by Spectral Interferometry," *Opt. Lett.* **26:** 1436–1438 (2001).
38. G. G. Paulus, F. Grabson, H. Walther, P. Villoresti, M. Nisoli, S. Stagira, E. Priori, and S. De Silvestri, "Absolute-Phase Phenomena in Photoionization with Few-Cycle Laser Pulses," *Nature* **414:** 182–184, (2001).
39. P. Antoine, A. L'Huillier, and M. Lewenstein, "Attosecond Pulse Trains Using High–Order Harmonics," *Phys. Rev. Lett.* **77**, 1234 (1996).
40. P. Tzallas, D. Charalambidis, N. A. Papadogiannis, K. Witte, and G. D. Tsakiris, "Direct Observation of Attosecond Light Bunching," *Nature* **426:** 267–271 (2003).
41. J. Mauritsson, P. Johnsson, E. Gustafsson, A. L'Huillier, K. J. Schafer, and M. B. Gaarde, "Attosecond Pulse Trains Generated Using Two Color Laser Fields," *Phys. Rev. Lett.* **97:** 013001 (2006).
42. G. Sanssone, E. Benedetti, F. Calegari, C. Vozzi, L. Avaldi, R. Flammini, L. Poletto, et al., "Isolated Single-Cycle Attosecond Pulses," *Science* **314:** 443 (2006).
43. Z. Chang, "Single Attosecond Pulse and xuv Supercontinuum in the High-Order Harmonic Plateau," *Phys. Rev. A* **70:** 043802 (2004).
44. H. Mashiko, S. Gilbertson, C. Li, S. D. Khan, M. M. Shakya, E. Moon, and Z. Chang, "Double Optical Gating of High-Order Harmonic Generation with Carrier-Envelope Phase Stabilized Lasers," *Phys Rev. Lett.* **100:** 103906 (2008).
45. R. Trebino, D. J. Kane, "Using Phase Retrieval to Measure the Intensity and Phase of Ultrashort Pulses: Frequency-Resolved Optical Gating," *J. Opt. Soc. Am. A* **10:** 1101 (1993).
46. A. Kosuge, T. Sekikawa, X. Zhou, T. Kanai, S. Adachi, and S. Watanabe, "Frequency-Resolved Optical Gating of Isolated Attosecond Pulses in the Extreme Ultraviolet," *Phys. Rev. Lett.* **97:** 263901 (2006).
47. R. Kienberger, M. Hentschel, M. Uiberacker, Ch. Spielmann, M. Kitzler, A. Scrinzi, M. Wieland, et al., "Steering Attosecond Electron Wave Packets with Light," *Science* **297:** 1144−1148 (2002).
48. J. Itatani, F. Quéré, G. L. Yudin, M. Yu. Ivanov, F. Krausz, and P. B. Corkum, "Attosecond Streak Camera," *Phys. Rev. Lett.* **88:** 173903 (2002).
49. Y. Mairesse, and F. Quéré, "Frequency-Resolved Optical Gating for Complete Reconstruction of Attosecond Bursts," *Phys. Rev. A* **71:** 011401(R) (2005).
50. J. Gagnon, E. Goulielmakis, V. S. Yakovlev, "The Accurate FROG Characterization of Attosecond Pulses from Streaking Measurements," *App. Phys. B* **92:** 25 (2008).